Sinterability and conductivity of barium doped aluminium lanthanum oxyapatite La$_{9.5}$Ba$_{0.5}$Si$_{5.5}$Al$_{0.5}$O$_{26.5}$ electrolyte of solid oxide fuel cells

Xiao Guo Cao[a], San Ping Jiang[b],*

[a] Faculty of Materials and Energy, Guangdong University of Technology, Guangzhou 510006, Guangdong, China
[b] Fuels and Energy Technology Institute & Department of Chemical Engineering, Curtin University, Perth, WA 6102, Australia

ARTICLE INFO

ABSTRACT

Apatite ceramics are interesting alternative solid oxide fuel cells (SOFCs) electrolytes because of their open structure for the transportation of oxide ions and their good chemical stability. This study reports the influence of barium doping on the microstructure, sinterability and oxide conductivity properties of the aluminium lanthanum oxyapatite La$_{9.5}$Ba$_{0.5}$Si$_{5.5}$Al$_{0.5}$O$_{26.5}$. SEM results show that lanthanum substitution with barium improves the sinterability of apatite ceramics. The barium doping also enhances the conductivity of the aluminium lanthanum silicates. The oxygen ion conductivity of La$_{9.5}$Ba$_{0.5}$Si$_{5.5}$Al$_{0.5}$O$_{26.5}$ sintered at 1600 °C is 2.21×10^{-2} S cm^{-1} at 800 °C, higher than 9.81×10^{-3} S cm^{-1} of La$_{10}$Si$_5$AlO$_{26.5}$ sample prepared under the same conditions. The results in the present study demonstrate that doping Ba on the La site for aluminium lanthanum oxyapatite reduces the sintering temperature and improves the ion conductivity. The enhancement of Ba dopant is mainly on the improvement of the densification and thus substantially reduced grain boundary resistance of aluminium lanthanum oxyapatite particularly at low temperatures

© 2012 Elsevier B.V. All rights reserved.

1. Introduction

Solid oxide fuel cell (SOFC) operating at intermediate temperatures of 600–800 °C is attracting world attention owing to its promising benefits of the increased long-term stability, wide range of material selection and possibility of using low cost processing techniques. However, reducing the operating temperature of SOFC also increases the polarization losses associated with the electrode and electrolyte reactions. Thus, one of the major challenges in the development of intermediate temperature SOFCs is to develop a solid oxide electrolyte material with a high conductivity to maintain the low electrolyte resistance during operation. Lanthanum silicate oxyapatite is emerging as new class of oxide ion conductors and a substantial level of oxygen ionic transport has been reported for apatite type phases A$_{10-y}$Si$_6$O$_{26\pm\delta}$, where A corresponds to rare-earth and alkaline-earth metal cations [1–13]. The apatite lattice consists of covalent SiO$_4$ tetrahedra and ionic-like La/O channels [4,7,14]. The A-site cations occupy cavities created by SiO$_4$ units with four distinct oxygen positions; additional oxygen sites form channels through the lattice. The open structure of lanthanum silicate apatite suggests that this material should be appropriate for the electrolyte applications for intermediate

temperature SOFCs. The apatite structured oxides have advantages of lower activation energy for ionic conduction as compared with conventional solid electrolytes [10,15,16]. High oxygen ion conductivity ($\sigma = 1.50 \times 10^{-3}$ S cm^{-1} at 500 °C and 3.46×10^{-2} S cm^{-1} at 800 °C) was also reported for La$_{10}$Si$_6$O$_{27}$ apatite electrolyte synthesized by a water-based gel-casting technique [17]. However, due to difficulties in sintering and different processing techniques, the conductivity values reported in the literature vary greatly, for example, from 8.4×10^{-5} to 4.3×10^{-3} S cm^{-1} at 500 °C for La$_{10}$Si$_6$O$_{27}$ [1,2,5].

The oxide conductivity in La$_{9.33}$Si$_6$O$_{26}$ is lower than that in La$_{10}$Si$_6$O$_{27}$, but higher than La$_8$Sr$_2$Si$_6$O$_{26}$ [4,6,18]. The simulation study [7] indicates that oxygen ion migration in La$_8$Sr$_2$Si$_6$O$_{26}$ is via a vacancy mechanism with a direct linear path, however, for La$_{9.33}$Si$_6$O$_{26}$, oxygen ion migration is via an interstitial mechanism with non-linear (sinusoidal-like) pathway along the c-axis channel. This suggests a significant role of interstitial migration and a possible improvement in the conductivity when apatite phases contain more than 26 oxygen ions per unit formula [5,7]. The simulations also demonstrate the importance of local cooperative relaxation of [SiO$_4$] tetrahedral (towards the vacant La sites) to assist in the facile conduction of oxygen interstitial ions. Slightly doped oxygen stoichiometric composition has been found to be favorable for the fabrication of highly conducting lanthanum silicate apatite [19]. In particular, an enhancement of the sinterability and ionic conduction was found in aluminium lanthanum oxyapatite, La$_{9.33+x/3}$Si$_{6-x}$Al$_x$O$_{26.5}$ [6,20–22].

Doping of $La_{10-x}(Si,Al)_6O_{26\pm\delta}$ with iron increased the total conductivity and sinterability [22–26]. The studies show an enhancement of the ionic conduction in the $La_{10-x}(Si,Al)_6O_{26\pm\delta}$ series, where Al doping is compensated by the La-site vacancies without oxygen content variations [6,22,24] or the oxygen excess without La-cation vacancies [25,27]. Experiments on alkaline earth doping studies in samples containing oxygen excess show that the conductivity of barium doped $La_9Ba(SiO_4)_6O_{2.5}$, which is cation stoichiometric but contains an oxygen excess, is high [28–30]. There are clear evidences that oxygen over-stoichiometry is responsible for the good oxide conductivity properties. An increase of conductivity was observed when lanthanum was partly substituted with an alkaline earth element and the conductivity increases with the dopant size. Arikawa et al. [31] reported the best conductivity on $La_{9.75}Sr_{0.25}Si_6O_{26.875}$ ($\sigma = 3.7 \times 10^{-2}$ S cm^{-1} at 800 °C), while for Slater and Sansam [32], best results were obtained on $La_9BaSi_6O_{26.5}$ with $\sigma = 1.3 \times 10^{-2}$ S cm^{-1} at 800 °C. A substitute of La with Ba (rBa^{2+} (VII) = 1.39 Å), whose radius is larger than Sr and La (rSr^{2+} (VII) = 1.21 Å, rLa^{3+} (VII/IX) = 1.06/1.20 Å), would lead to enhanced conductivity [32–34]. Thus it would be interesting to study the effect of Ba doping on the sintering and conduction properties of aluminium lanthanum oxyapatite.

As shown by Nojiri et al. [33], the conductivity of $La_{10-x}Ba_xSi_6O_{27-x/2}$ exhibited a maximum around $x = 0.5$–0.6. Thus, Ba doped aluminium lanthanum apatite with composition $La_{9.5}Ba_{0.5}Si_{5.5}Al_{0.5}O_{26.5}$ was selected for this study. The undoped aluminium lanthanum oxyapatite $La_{10}Si_5AlO_{26.5}$ was also studied under identical conditions. The effect of substitution of La with Ba on the sinterability and conductivity were studied by SEM and electrochemical impedance analysis. The results show that doping Ba on the La site improves the sinterability and conductivity as compared to the undoped aluminium lanthanum oxyapatite.

2. Experimental

2.1. Synthesis of $La_{9.5}Ba_{0.5}Si_{5.5}Al_{0.5}O_{26.5}$ and $La_{10}Si_5AlO_{26.5}$ powders

High purity La_2O_3, SiO_2, Al_2O_3 and $BaCO_3$ (all from Sigma–Aldrich) were used as the starting materials. The powders were weighed in appropriate ratio to elaborate the compounds $La_{9.5}Ba_{0.5}Si_{5.5}Al_{0.5}O_{26.5}$ and $La_{10}Si_5AlO_{26.5}$ and mixed in plastic vessels for 24 h. Isopropanol and zirconia balls were used as solvent and media, respectively. After drying, the powders were calcined between 1000 and 1400 °C for 10 h at 100 °C interval in air, and the powders were dispersed in isopropanol and pulverized in a ball-mill using an Y_2O_3-stabilized zirconia (YSZ) ball medium.

2.2. Characterization

As-synthesized apatite powders were pressed uniaxially into pellets and bars under a pressure of 150 MPa and sintered at 1450, 1500, 1550 and 1650 °C, respectively for 4 h in air. Phase formation of the apatite powders synthesized by solid state reaction method was determined by X-ray diffraction (XRD, Philips MPD 1880) using Cu K$_\alpha$ radiation at room temperature. The microstructure of $La_{9.5}Ba_{0.5}Si_{5.5}Al_{0.5}O_{26.5}$ and $La_{10}Si_5AlO_{26.5}$ pellets was examined by scanning electron microscope (SEM, JSM-5600/LV). The bulk densities of the sintered apatites were obtained from the mass and geometric dimensions of the pellet samples.

The sintered pellets with ~9 mm in diameter and 1.5 mm in thickness were used for the electrochemical impedance analysis. Silver paste (Ferro Corporation USA) was painted onto both sides of the samples as the electrodes. For the impedance measurements, a Solartron 1260 frequency response analyzer was used over the frequency range of 1 MHz to 1 Hz. The measurements were made in 50 °C interval in air between 300 °C and 800 °C.

3. Results and discussion

3.1. XRD and microstructure analysis

The XRD patterns of $La_{10}Si_5AlO_{26.5}$ and $La_{9.5}Ba_{0.5}Si_{5.5}Al_{0.5}O_{26.5}$ obtained at different temperatures (1000, 1100, 1200, 1300 and 1400 °C) are shown in Fig. 1. As seen from Fig. 1, a secondary phase, La_2SiO_5 was found in both $La_{9.5}Ba_{0.5}Si_{5.5}Al_{0.5}O_{26.5}$ and $La_{10}Si_5AlO_{26.5}$ powders synthesized at the temperatures of
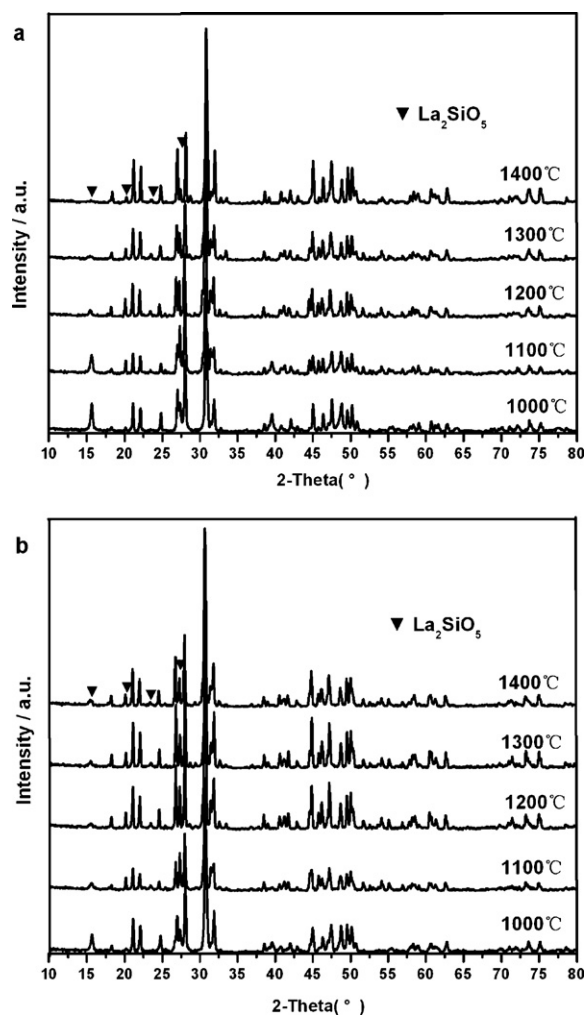
Fig. 1. XRD patterns of (a) $La_{10}Si_5AlO26.5$ and (b) $La9.5Ba0.5Si5.5Al0.5O26.5$ powders. The apatite electrolyte powders were calcined at 1000, 1100, 1200, 1300 and 1400 °C for 10 h in air.

1000–1400 °C by solid state reaction method. This indicates that it would be difficult to obtain a homogeneous mixture of the oxide precursors with solid state reaction route, consistent with that reported by Tao and Irvine [5] and Jiang et al. [17]. The XRD data also reveals that the intensity of the minor La_2SiO_5 phase was reduced with the increase of calcined temperature. According to the La_2O_3/SiO_2 phase diagram [35]: La_2SiO_5 and $La_2Si_2O_7$ phases are more stable than apatite below 1600 °C. As shown by Tao et al., La_2SiO_5 is difficult to remove once it is formed during the solid-state synthesis [5]. Thus in the present study, apatite powders were pre-calcined at 1300 °C.

Fig. 2 shows the fractured cross-section SEM micrographs of $La_{10}Si_5AlO_{26.5}$ and $La_{9.5}Ba_{0.5}Si_{5.5}Al_{0.5}O_{26.5}$ apatite pellets sintered at different temperatures. The powders were calcined at 1300 °C for 10 h in air. SEM observation shows that $La_{10}Si_5AlO_{26.5}$ electrolyte samples are very porous and the porosity of $La_{10}Si_5AlO_{26.5}$ apatites decreases with the increase of sintering temperature (Fig. 2a). On the other hand, $La_{9.5}Ba_{0.5}Si_{5.5}Al_{0.5}O_{26.5}$ apatite pellets show a much denser and compact structures with low porosity (Fig. 2b). The porosity of the Ba doped aluminium lanthanum oxyapatite $La_{9.5}Ba_{0.5}Si_{5.5}Al_{0.5}O_{26.5}$ is significantly smaller than that of undoped $La_{10}Si_5AlO_{26.5}$ samples sintered at temperature ranges from 1450 to 1600 °C. The significant difference of $La_{10}Si_5AlO_{26.5}$ and $La_{9.5}Ba_{0.5}Si_{5.5}Al_{0.5}O_{26.5}$ apatite in microstructure can also be seen clearly from the thermally etched samples. Fig. 3 shows

a) $La_{10}Si_5AlO_{26.5}$ b) $La_{9.5}Ba_{0.5}Si_{5.5}Al_{0.5}O_{26.5}$
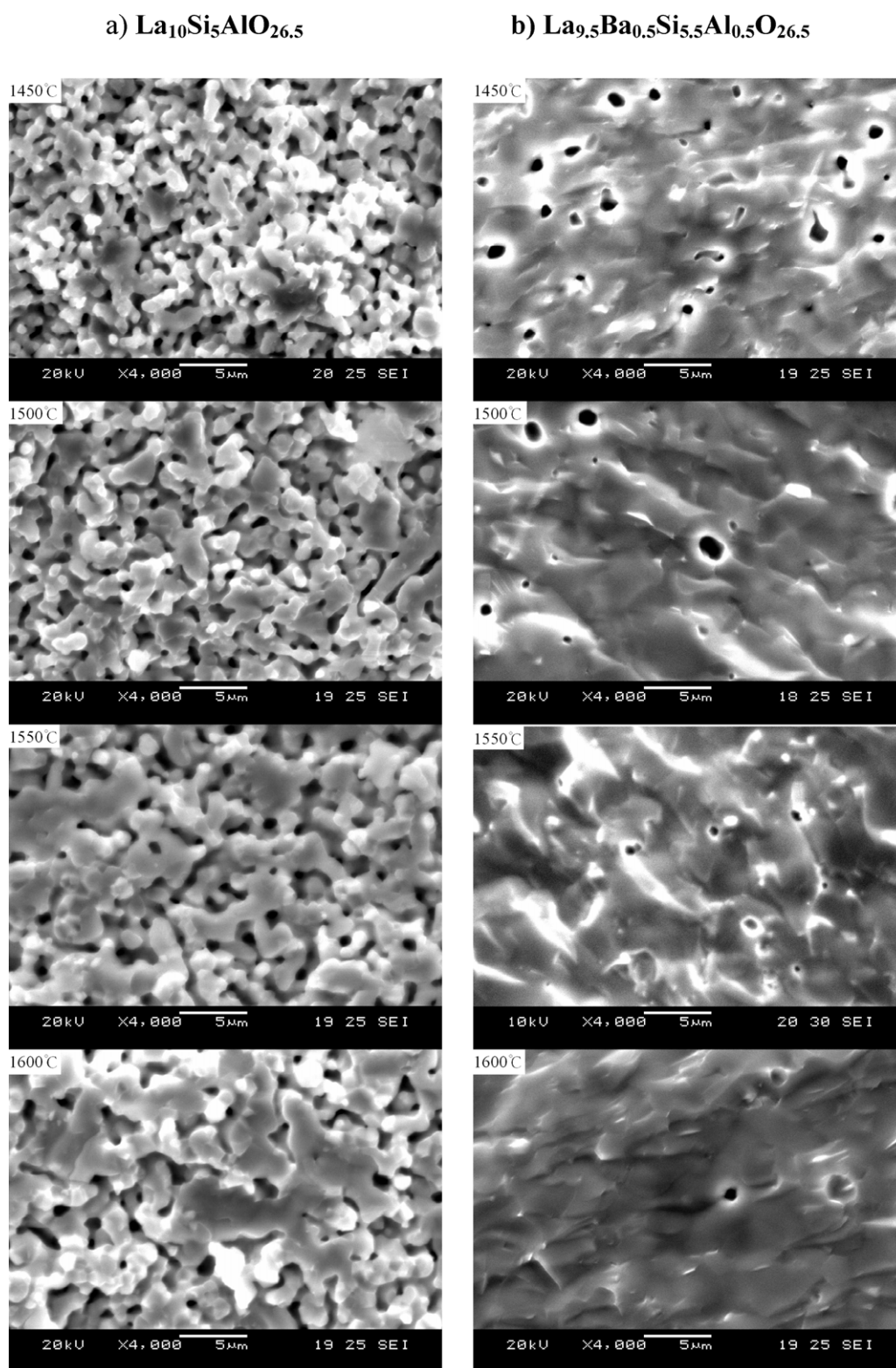
Fig. 2. SEM micrographs of fractured cross-sections of (a) La10Si5AlO26.5 and (b) La9.5Ba0.5Si5.5Al0.5O26.5 apatite pellets sintered at 1450, 1500, 1550 and 1600 °C for 4 h in air. The apatite powders were calcined at 1300 °C for 10 h in air.

the SEM micrographs of $La_{10}Si_5AlO_{26.5}$ and $La_{9.5}Ba_{0.5}Si_{5.5}Al_{0.5}O_{26.5}$ apatite pellets sintered at 1550 °C. The powders were calcined at 1300 °C for 10 h in air and samples were thermally etched at 1500 °C. There are significant number of pores formed on the surface of $La_{10}Si_5AlO_{26.5}$ (Fig. 3a) as compared with $La_{9.5}Ba_{0.5}Si_{5.5}Al_{0.5}O_{26.5}$ apatite (Fig. 3b). This indicates that doping

Ba on the La site of aluminium lanthanum apatite $La_{10}Si_5AlO_{26.5}$ significantly benefits the sintering process. As seen from Fig. 3b, glassy phase was found on the surface of the $La_{9.5}Ba_{0.5}Si_{5.5}Al_{0.5}O_{26.5}$ sample. The reasons of the formation of glassy phase are not clear at this stage. However, from the conductivity measurements, the formation of such glassy phase on the electrolyte surface appears to have
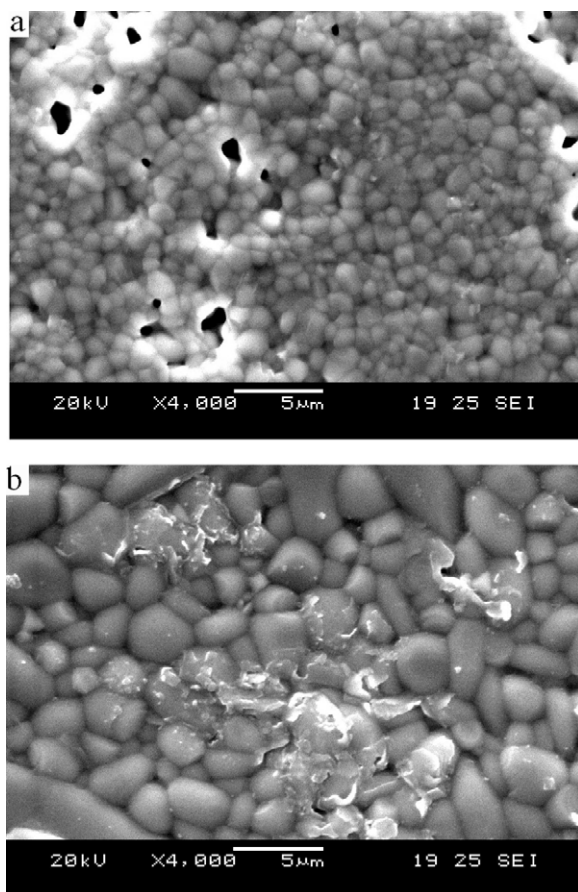
Fig. 3. SEM micrographs of the surface of thermally etched (a) La10Si5AlO26.5 and (b) La9.5Ba0.5Si5.5Al0.5O26.5 apatite pellets. The samples were sintered at 1550 °C and thermally etched at 1500 °C.

Fig. 4. Bulk density of the La9.5Ba0.5Si5.5Al0.5O26.5 and La10Si5AlO26.5 ceramics sintered at 1450, 1500, 1550 and 1600 °C for 4 h in air. The apatite powders were calcined at 1300 °C for 10 h in air.

little effect on the oxide ion conduction (see following section). The size of $La_{9.5}Ba_{0.5}Si_{5.5}Al_{0.5}O_{26.5}$ grains is in the range 1.7–2.5 μm, significantly larger than that 0.8–1.1 μm of $La_{10}Si_5AlO_{26.5}$. The relatively large grains of $La_{9.5}Ba_{0.5}Si_{5.5}Al_{0.5}O_{26.5}$ again indicate that doping Ba on the La site of apatite-type $La_{10}Si_5AlO_{26.5}$ significantly enhances the sintering and densification process.

The significant differences in the microstructure of the $La_{9.5}Ba_{0.5}Si_{5.5}Al_{0.5}O_{26.5}$ and $La_{10}Si_5AlO_{26.5}$ ceramics are also indicated by the bulk density of the $La_{9.5}Ba_{0.5}Si_{5.5}Al_{0.5}O_{26.5}$ and $La_{10}Si_5AlO_{26.5}$ ceramics sintered at different temperature, as shown in Fig. 4. At the sintering temperature of 1450 °C, the bulk density of $La_{10}Si_5AlO_{26.5}$ is 3.51 g cm^{-3}, which is significantly smaller than 5.10 g cm^{-3} of $La_{9.5}Ba_{0.5}Si_{5.5}Al_{0.5}O_{26.5}$. As evident from Fig. 4, the bulk density increases with the sintering temperature. The bulk density of $La_{9.5}Ba_{0.5}Si_{5.5}Al_{0.5}O_{26.5}$ samples is significantly higher than that of $La_{10}Si_5AlO_{26.5}$ samples sintered at the identical temperatures. The results are consistent with the SEM observation. This again indicates that doping Ba is advantageous in enhancing the densification as compared to the undoped aluminium lanthanum silicate $La_{10}Si_5AlO_{26.5}$.

3.2. Conductivity properties

The conductivities of $La_{9.5}Ba_{0.5}Si_{5.5}Al_{0.5}O_{26.5}$ and $La_{10}Si_5AlO_{26.5}$ sintered at different temperatures were investigated by electrochemical impedance spectroscopy in temperature range of 300–800 °C. Fig. 5 shows the complex impedance plots of $La_{10}Si_5AlO_{26.5}$ and $La_{9.5}Ba_{0.5}Si_{5.5}Al_{0.5}O_{26.5}$ apatites sintered at 1550 °C, measured at 300, 500 and 800 °C. The apatite powders

were calcined at 1300 °C for 10 h in air. The impedance responses of apatite oxides change significantly with the measuring temperature. And the impedance of $La_{10}Si_5AlO_{26.5}$ is significantly higher than that of $La_{9.5}Ba_{0.5}Si_{5.5}Al_{0.5}O_{26.5}$ at the same testing temperatures. The impedance response of $La_{10}Si_5AlO_{26.5}$ and $La_{9.5}Ba_{0.5}Si_{5.5}Al_{0.5}O_{26.5}$ materials measured at 800 °C exhibits one depressed semicircle. The impedance curves at 500 °C consist of two distorted overlap semicircles at high and low frequencies. This distorted semicircle arises from a bulk contribution at high frequencies overlapped by another semicircle at low frequencies, characteristic of the grain boundary response. The impedance arc at the low frequencies of the $La_{10}Si_5AlO_{26.5}$ apatite oxides is substantially bigger than that of $La_{9.5}Ba_{0.5}Si_{5.5}Al_{0.5}O_{26.5}$ apatite ceramics. As shown in Fig. 3, the average grain size of $La_{10}Si_5AlO_{26.5}$ apatite is significantly smaller than that of $La_{9.5}Ba_{0.5}Si_{5.5}Al_{0.5}O_{26.5}$ apatite, indicating the high grain boundaries of the undoped aluminium lanthanum apatite $La_{10}Si_5AlO_{26.5.}$ Thus the high grain boundary resistance of $La_{10}Si_5AlO_{26.5}$ apatite oxide is most likely due to the much smaller grain size of $La_{10}Si_5AlO_{26.5}$ as compared with that of $La_{9.5}Ba_{0.5}Si_{5.5}Al_{0.5}O_{26.5}$ apatite ceramics. At 300 °C, the semicircle at high frequency almost disappears, which indicates that the domination of bulk resistance to the total resistivity of apatite electrolyte is negligible. As shown in Fig. 5 for the impedance curves at different temperatures, the grain boundary resistance increases visibly with the decrease of temperature, which suggests considerable grain boundary contribution to the total resistivity of apatite electrolyte at low temperatures. This in turn indicates that the enhancement of lanthanum substitution with barium in aluminium lanthanum oxygapatite is primarily due to the improvement of the densification and thus substantially reduced grain boundary resistance of the aluminium lanthanum oxygapatite particularly at low temperatures. However, the separation of the bulk and grain boundary contributions from the impedance curves is difficult due to the substantial overlapping of the impedance arcs. This appears to be a general problem for the apatite systems [4]. Thus, the conductivities reported in this paper are the total conductivity.

Fig. 6 shows the Arrhenius activation energy plots of $La_{10}Si_5AlO_{26.5}$ and $La_{9.5}Ba_{0.5}Si_{5.5}Al_{0.5}O_{26.5}$ apatite samples. From the slope, activation energy of the oxide conductivity was calculated. Table 1 lists the conductivity and activation energy of $La_{9.5}Ba_{0.5}Si_{5.5}Al_{0.5}O_{26.5}$ and $La_{10}Si_5AlO_{26.5}$ apatite ceramics as a function of sintering temperatures. It can be seen that the
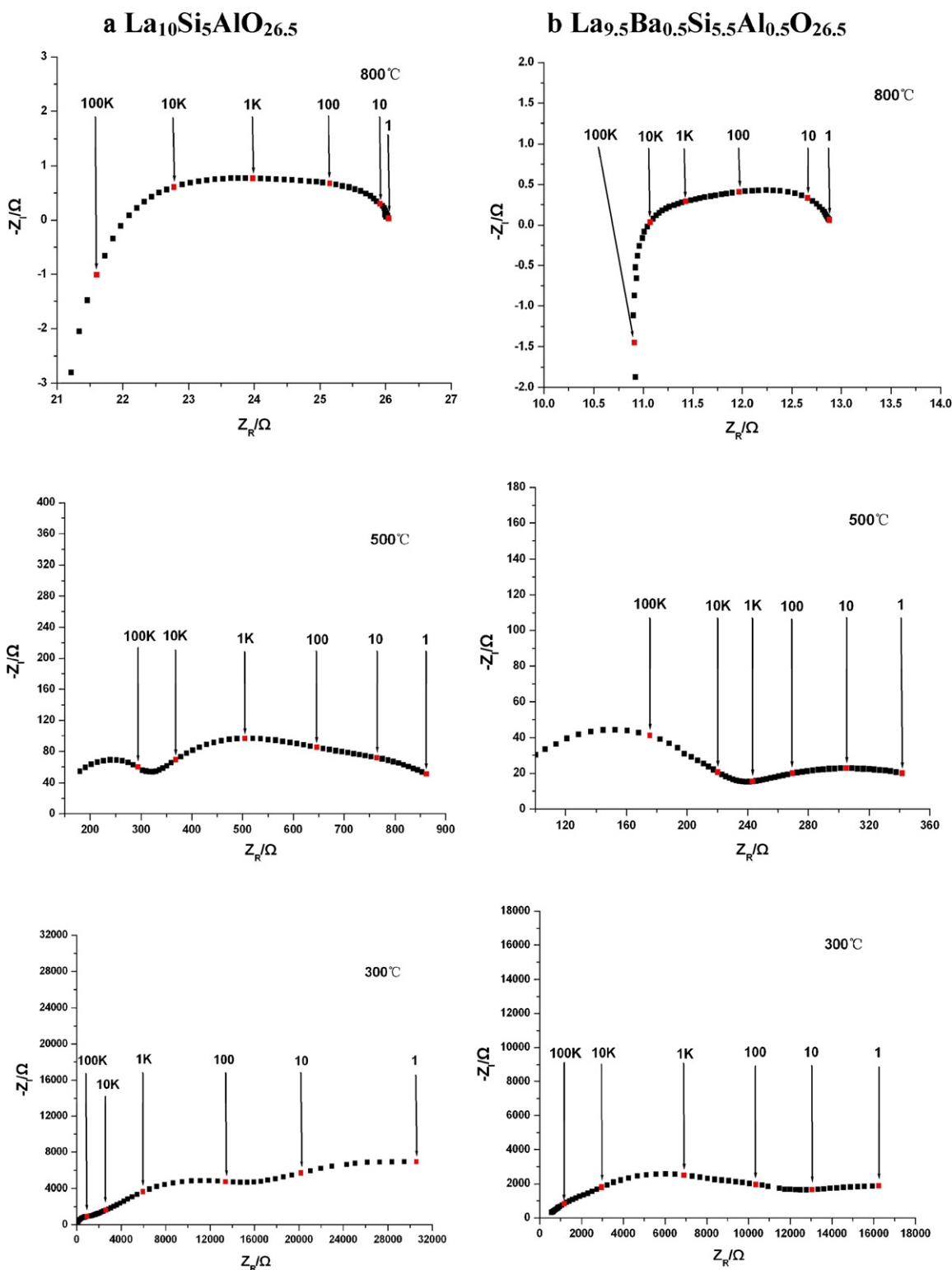
Fig. 5. Complex impedance plots of (a) La10Si5AlO26.5 and (b) La9.5Ba0.5Si5.5Al0.5O26.5 apatite electrolytes, measured at 300, 500 and 800 °C. The apatite samples were sintered at 1550 °C for 4 h in air and the numbers in the figure are frequencies in Hz.

conductivity of $La_{10}Si_5AlO_{26.5}$ is generally lower than that of $La_{9.5}Ba_{0.5}Si_{5.5}Al_{0.5}O_{26.5}$ and the conductivity of both $La_{10}Si_5AlO_{26.5}$ and $La_{9.5}Ba_{0.5}Si_{5.5}Al_{0.5}O_{26.5}$ significantly increases with the sintering temperatures. For example, the conductivity of $La_{10}Si_5AlO_{26.5}$ sintered at 1600 °C is 9.81×10^{-3} S cm^{-1} at 800 °C, which is significantly lower than 2.21×10^{-2} S cm^{-1} at 800 °C obtained on $La_{9.5}Ba_{0.5}Si_{5.5}Al_{0.5}O_{26.5}$ sintered at the same temperature. This

indicates that substitution of lanthanum with barium enhances the conductivity properties of aluminium lanthanum oxyapatite oxide electrolytes. The oxide conductivity of $La_{9.5}Ba_{0.5}Si_{5.5}Al_{0.5}O_{26.5}$ in this study ($\sigma = 2.21 \times 10^{-2}$ S cm^{-1} at 800 °C) is slightly higher than 1.3×10^{-2} S cm^{-1} at 800 °C reported on $La_9BaSi_6O_{26.5}$ [32].

The activation energy for the ionic conductivity of $La_{9.5}Ba_{0.5}Si_{5.5}Al_{0.5}O_{26.5}$ apatite electrolytes is in the range of

Table 1
Conductivity and activation energy of $La_{9.5}Ba_{0.5}Si_{5.5}Al_{0.5}O_{26.5}$ and $La_{10}Si_5AlO_{26.5}$ apatite ceramics as a function of sintering temperatures.

Sintering temperature (°C)	Conductivity (S cm⁻¹)						E_a (kJ mol⁻¹)
	300	400	500	600	700	800	
$La_{10}Si_5AlO_{26.5}$							
1600	8.09×10^{-6}	7.29×10^{-5}	3.96×10^{-4}	1.52×10^{-3}	4.91×10^{-3}	9.81×10^{-3}	80.61
1550	3.92×10^{-6}	3.49×10^{-5}	2.10×10^{-4}	8.95×10^{-4}	4.54×10^{-3}	8.84×10^{-3}	87.16
1500	2.31×10^{-6}	2.50×10^{-5}	1.57×10^{-4}	6.06×10^{-4}	1.95×10^{-3}	4.07×10^{-3}	83.89
1450	1.55×10^{-6}	1.85×10^{-5}	1.27×10^{-4}	5.27×10^{-4}	1.55×10^{-3}	3.96×10^{-3}	87.33
$La_{9.5}Ba_{0.5}Si_{5.5}Al_{0.5}O_{26.5}$							
1600	4.53×10^{-6}	5.73×10^{-5}	5.18×10^{-4}	2.84×10^{-3}	1.16×10^{-2}	2.21×10^{-2}	97.27
1550	1.64×10^{-5}	1.43×10^{-4}	8.44×10^{-4}	3.17×10^{-3}	8.82×10^{-3}	1.82×10^{-2}	79.80
1500	3.58×10^{-6}	4.32×10^{-5}	3.49×10^{-4}	1.73×10^{-3}	6.49×10^{-3}	1.28×10^{-2}	93.26
1450	9.07×10^{-7}	1.66×10^{-5}	1.38×10^{-4}	8.22×10^{-4}	3.40×10^{-3}	9.50×10^{-3}	102.18
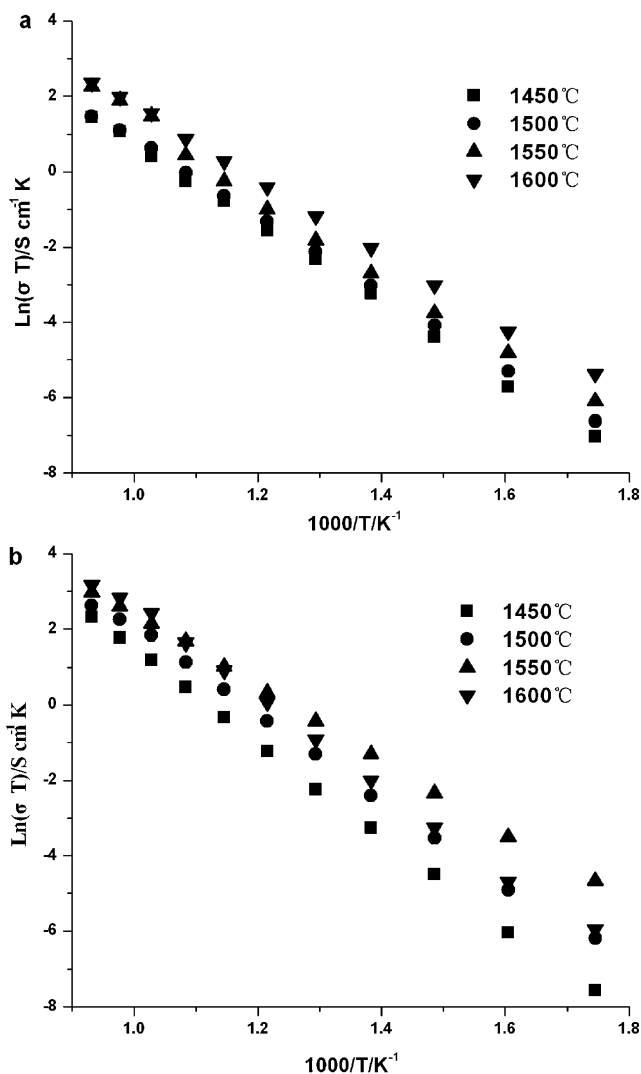
Fig. 6. Arrhenius plots of oxide conductivity of (a) La10Si5AlO26.5 and (b) La9.5Ba0.5Si5.5Al0.5O26.5 apatite samples. Apatite electrolyte specimens were prepared from the powders calcined at 1300 °C and sintered at 1450, 1500, 1550 and 1600 °C.

4. Conclusions

$La_{9.5}Ba_{0.5}Si_{5.5}Al_{0.5}O_{26.5}$ and $La_{10}Si_5AlO_{26.5}$ apatite samples were synthesized by using a conventional solid state reaction process. SEM and density measurements revealed that doping Ba on the La site of aluminium lanthanum oxyapatite-type $La_{10}Si_5AlO_{26.5}$ benefits significantly the sintering and densification process. $La_{9.5}Ba_{0.5}Si_{5.5}Al_{0.5}O_{26.5}$ apatite shows significantly better microstructure and high bulk density as compared with that of $La_{10}Si_5AlO_{26.5}$ apatite prepared under identical conditions. The effect of sintering temperatures on the conductivity of $La_{9.5}Ba_{0.5}Si_{5.5}Al_{0.5}O_{26.5}$ was investigated in detail in the temperature range between 300 and 800 °C by the complex impedance spectroscopy. The conductivity studies show that $La_{9.5}Ba_{0.5}Si_{5.5}Al_{0.5}O_{26.5}$ has a better conductivity than $La_{10}Si_5AlO_{26.5}$. The conductivity of $La_{9.5}Ba_{0.5}Si_{5.5}Al_{0.5}O_{26.5}$ sintered at 1600 °C is 2.21×10^{-2} S cm⁻¹ at 800 °C, significantly higher than 9.81×10^{-3} S cm⁻¹ of $La_{10}Si_5AlO_{26.5}$ sintered at the same temperature. The results in the present study demonstrate that doping Ba on the La site for apatite-type $La_{10}Si_5AlO_{26.5}$ significantly reduces the sintering temperature and improves the ion conductivity. The enhancement of lanthanum substitution with barium in aluminium lanthanum oxygapatite is most likely due to the improvement of the densification and thus substantially reduced grain boundary resistance of the apatite particularly at low temperatures.

References

[1] S. Nakayama, T. Kageyama, H. Aono, Y. Sadaoka, J. Mater. Chem. 5 (1995) 1801–1805.
[2] S. Nakayama, M. Sakamoto, J. Eur. Ceram. Soc. 18 (1998) 1413–1418.
[3] S. Nakayama, M. Sakamoto, M. Higuchi, K. Kodaira, M. Sato, S. Kakita, T. Suzuki, K. Itoh, J. Eur. Ceram. Soc. 19 (1999) 507–510.
[4] J.E.H. Sansom, D. Richings, P.R. Slater, Solid State Ionics 139 (2001) 205–210.
[5] S.W. Tao, J.T.S. Irvine, Mater. Res. Bull. 36 (2001) 1245–1258.
[6] E.J. Abram, D.C. Sinclair, A.R. West, J. Mater. Chem. 11 (2001) 1978–1979.
[7] J.R. Tolchard, M.S. Islam, P.R. Slater, J. Mater. Chem. 13 (2003) 1956–1961.
[8] E. Bechade, I. Julien, T. Iwata, O. Masson, P. Thomas, E. Champion, K. Fukuda, J. Eur. Ceram. Soc. 28 (2008) 2717–2724.
[9] A. Chesnaud, G. Dezanneau, C. Estournes, C. Bogicevic, F. Karolak, S. Geiger, G. Geneste, Solid State Ionics 179 (2008) 1929–1939.
[10] S.H. Jo, P. Muralidharan, D.K. Kim, Electrochim. Acta 54 (2009) 7495–7501.
[11] Y. Higuchi, M. Sugawara, K. Onishi, M. Sakamoto, S. Nakayama, Ceram. Int. 36 (2010) 955–959.
[12] A. Mineshige, T. Nakao, Y. Ohnishi, R. Sakamoto, Y. Daiko, M. Kobune, T. Yazawa, H. Yoshioka, T. Fukutsuka, Y. Uchimoto, J. Electrochem. Soc. 157 (2010) B1465–B1470.
[13] M.S. Islam, J.R. Tolchard, P.R. Slater, Chem. Commun. (2003) 1486–1487.
[14] M.S. Islam, Philos. Trans. R. Soc. A Math. Phys. Eng. Sci. 368 (2010) 3255–3267.

79–102 kJ mol⁻¹, slightly higher than 80–87 kJ mol⁻¹ observed on $La_{10}Si_5AlO_{26.5}$ apatite electrolytes. Shaula et al. [22] reported that the activation energy for the ionic conductivity of $La_{10}Si_5AlO_{26.5}$ sintered at 1650–1700 °C for 10 h is 56 ± 3 kJ mol⁻¹, which is smaller than the values observed in this study. This may be related to difference in the preparation process and higher sintering temperatures as reported in [22].

[15] L. Leon-Reina, E.R. Losilla, M. Martinez-Lara, S. Bruque, A. Llobet, D.V. Shep-tyakov, M.A.G. Aranda, J. Mater. Chem. 15 (2005) 2489–2498.
[16] A. Jones, P.R. Slater, M.S. Islam, Chem. Mater. 20 (2008) 5055–5060.
[17] S.P. Jiang, L. Zhang, H.Q. He, R.K. Yap, Y. Xiang, J. Power Sources 189 (2009) 972–981.
[18] Y. Masubuchi, M. Higuchi, H. Katase, T. Takeda, S. Kikkawa, K. Kodaira, S. Nakayama, Solid State Ionics 166 (2004) 213–217.
[19] A. Mineshige, Y. Ohnishi, R. Sakamoto, Y. Daiko, M. Kobune, T. Yazawa, H. Yoshioka, T. Nakao, T. Fukutsuka, Y. Uchimoto, Solid State Ionics 192 (2011) 195–199.
[20] L. Leon-Reina, J.M. Porras-Vazquez, E.R. Losilla, M.A.G. Aranda, Solid State Ionics 177 (2006) 1307–1315.
[21] I. Santacruz, J.M. Porras-Vazquez, E.R. Losilla, M. Isabel Nieto, R. Moreno, M.A.G. Aranda, J. Am. Ceram. Soc. 94 (2011) 224–230.
[22] A.L. Shaula, V.V. Kharton, F.M.B. Marques, J. Solid State Chem. 178 (2005) 2050–2061.
[23] A.L. Shaula, V.V. Kharton, F.M.B. Marques, Presented at the 15th International Conference on Solid State Ionics, Baden Baden, Germany, 2006.
[24] A.L. Shaula, V.V. Kharton, J.C. Waerenborgh, D.P. Rojas, E. Tsipis, N.P. Vyshatko, M. Patrakeev, F.M.B. Marques, Mater. Res. Bull. 39 (2004) 763–773.
[25] S. Chefi, A. Madani, H. Boussetta, C. Roux, A. Hammou, J. Power Sources 177 (2008) 464–469.
[26] V.V. Kharton, A.L. Shaula, M.V. Patrakeev, J.C. Waerenborgh, D.P. Rojas, N.P. Vyshatko, E.V. Tsipis, A.A. Yaremchenko, F.M.B. Marques, J. Electrochem. Soc. 151 (2004) A1236–A1246.
[27] E.V. Tsipis, V.V. Kharton, J.R. Frade, Electrochim. Acta 52 (2007) 4428–4435.
[28] P.R. Slater, J.E.H. Sansam, Presented at the 5th International Conference on Solid State Chemistry, Bratislava, Slovakia, 2002.
[29] Y. Otsuka, S. Fujihara, J. Electrochem. Soc. 154 (2007) J335–J340.
[30] S. Guillot, S. Beaudet-Savignat, S. Lambert, P. Roussel, R.-N. Vannier, Solid State Ionics 185 (2011) 18–26.
[31] H. Arikawa, H. Nishiguchi, T. Ishihara, Y. Takita, Solid State Ionics 136 (2000) 31–37.
[32] P.R. Slater, J.E.H. Sansam, Solid State Chemistry V, vol. 90–91, Trans Tech Pub-lications Ltd, Zurich-Uetikon, 2003, pp. 195–200.
[33] Y. Nojiri, S. Tanase, M. Iwasa, H. Yoshioka, Y. Matsumura, T. Sakai, J. Power Sources 195 (2010) 4059–4064.
[34] L. Zhang, H.Q. He, H.W. Wu, C.Z. Li, S.P. Jiang, Int. J. Hydrogen Energy 36 (2011) 6862–6874.
[35] J. Felsche, J. Solid State Chem. 5 (1972) 266–270.